Optical and Quantum Electronics 12 (1980) 231–235

X-ray production by a laser plasma in a strong electric field

S. G. DINEV, Ch. I. RADEV,* K. V. STAMENOV, K. A. STANKOV
Department of Physics, Sofia University, 1126 Sofia, Bulgaria

Received 23 November 1979

The X-ray emission of a laser plasma from metal targets in a 26 kV cm^{-1} electric field is investigated experimentally. A substructure of the X-ray pulse, corresponding to the laser pulse train period is found. The spectrum of the radiation in the range 2–25 keV is measured.

1. Introduction

In a previous paper we have reported the enhancement, by several orders of magnitude, of X-ray emission when picosecond laser pulses are focused onto a solid target in a strong longitudinal electric field [1]. This effect was first observed photographically in [2]. Studying the X-ray dynamics we have observed three pulses with different amplitudes and spectral characteristics.

In this paper we report on the selection of a single X-ray pulse having a substructure with a period corresponding to the pumping laser pulse train period. Using a filter technique the spectrum of this pulse was measured.

2. Single X-ray pulse selection and testing

The experimental arrangement for the measurements is described in detail in [1]. Modifications to the target vacuum chamber allowed some hypotheses to be proved. The 0.6 mm thick Be windows of the camera and scintillator–photomultiplier system used in the previous experiment were replaced by 0.2 mm thick Be foil. The electric field in the interelectrode gap was increased up to 26 kV cm^{-1}. A Tektronix 7633 oscilloscope with a 7A24 plug-in was used instead of a Tektronix 466.

The first modification of the target arrangement is shown in Fig. 1a. The aim was to prove the mechanism for the production of the second X-ray pulse (see Fig. 3 in [1]). When the laser plasma is formed, ions are accelerated toward the opposite aluminium electrode E and produce electron emission. The electrons from E, accelerated back to the positive target T caused the emission of X-ray burst. The first indication of the mechanism is the pulse delay τ_2 dependence on the applied voltage U, $\tau_2 \propto U^{-0.48}$, which, within the experimental error corresponds to the time of flight of ions. In order to check it, a glass plate, P in Fig. 1a, was inserted in front of the aluminium electrode E to transmit the laser radiation at 530 nm and to stop the ion beam bombardment on E. The ion-electron emission from glass is negligible [3]. As seen in Fig. 2a the second pulse essentially disappeared and from now we shall deal with the first X-ray pulse shown on the oscilloscope trace. The same result was obtained with a teflon plate having an 8 mm diameter orifice in the centre.

In order to find out whether the first pulse is caused by bombardment of electrons, derived from the electrode E under the action of fast electrons and v.u.v. photons from the plasma, the target chamber was additionally modified, Fig. 1b. As seen in Fig. 1b, a 1 × 1 mm brass grid was placed on the glass plate surface. A negative voltage U_g with a magnitude of up to 2 kV with respect to the ground was applied to the grid. The electric field of the grid should stop the electrons emitted due to bombardment or v.u.v. irradiation. However, the amplitude of the X-ray pulse remained constant. The change of the grid voltage polarity had no effect on the X-ray emission. A 6 mm aperture teflon diaphragm D in the middle of the interelectrode gap also had no effect.

* Present address: Applied Physics Laboratory, Bulgarian Academy of Sciences, Plovdiv.

0306–8919/80/030231–05$02.50/0

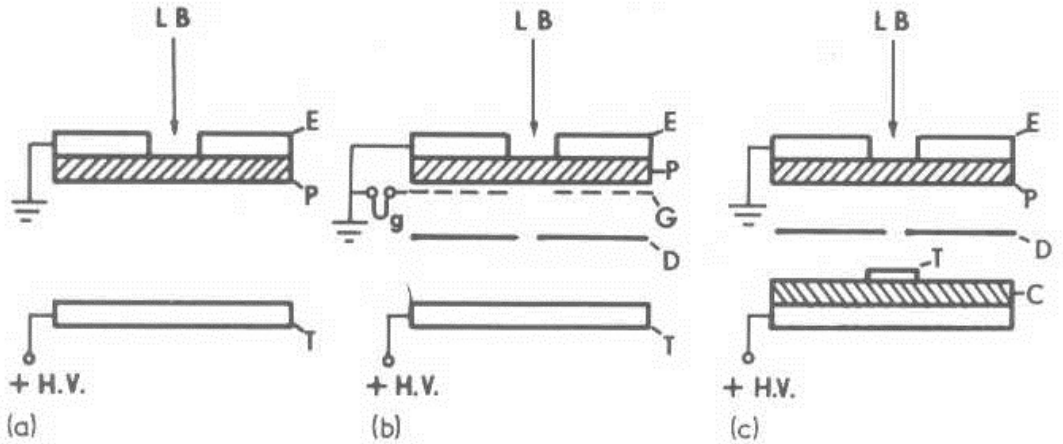

Figure 1 The target chamber arrangements for X-ray pulse selection and testing. T, target; E, Al electrode; P, 0.1 mm glass plate; G, 1 × 1 mm grid; *Ug*, grid voltage; D, 6 mm teflon diaphragm; C, ceramic plate; LB, laser beam.

The last target arrangement is depicted in Fig. 1c. The target area in this case is 25 times smaller, and the 0.5 mm thick ceramic plate C isolates the target material electrically from the high voltage. No change of the amplitude of the X-ray pulse was observed. These results, in our view, show clearly that the X-ray production is not due to accelerated electrons originated from the opposite electrode E.

The form and the amplitude of the X-ray pulse was investigated by changing the target material. Metal foils of approximately 1 mm thickness of Al ($Z = 13$), Ni ($Z = 28$), Cu ($Z = 29$), Mo ($Z = 42$) and W ($Z = 74$) were employed, where Z is the atomic number. As seen in Fig. 2b, a modulation of the pulse is presented with a period of 10 ns, corresponding to the laser pulse train period. A 2 mm thick Pb plate completely stops the X-ray beam. The amplitude of the interfering electrical noise is less than 5 mV. The observed modulation can be explained by the increase in Be window transmission (compared to the previous experiment) of the softer spectral components. Moreover, a trend of increasing the modulation depth with higher Z-numbers was noticed. In our view, the modulation depth is limited by the resolution capability of the scintillator–photomultiplier–oscilloscope system.

The pinhole camera [1] measurements revealed a similar point-like emitting source, as described previously. The spectrum of the pulse was measured using the filter technique. Al foils with thicknesses ranging from 20 μm to 1 mm were placed in front of the detection system and the signal attenuation recorded. An average of 15 shots was taken for each foil thickness.

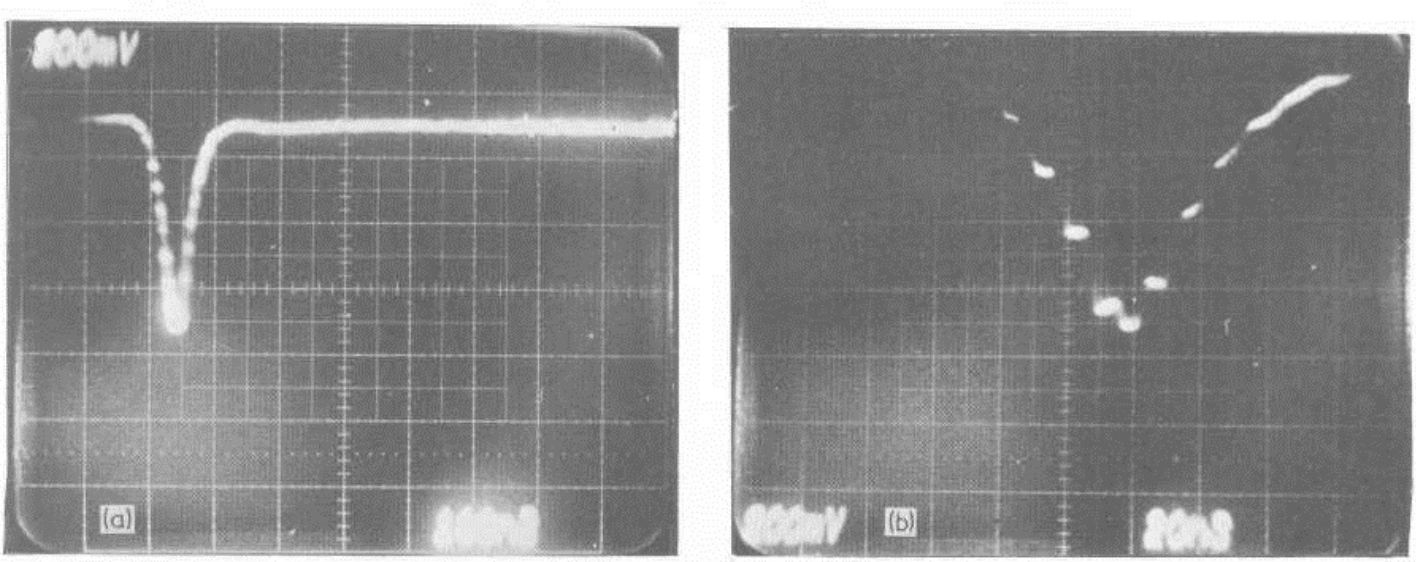

Figure 2 Oscilloscope trace of the single X-ray pulse: (a) first X-ray pulse selected, horizontal scale 100 ns div^{-1}; (b) 10 ns period substructure of the pulse, horizontal scale 20 ns div^{-1}. Vertical scale 200 mV div^{-1}.

3. Spectrum analysis

In order to calculate the spectral distribution of the X-ray emission, a method, described in [4], was applied, modified according to our experimental conditions. Suppose the X-ray radiation with a spectral distribution function $S_1(E)$ is attenuated by an absorber having a thickness x and absorption coefficient μ. The integral energy $W(x)$ received by the detector is

$$W(x) = \int_0^\infty S(E) \exp [-\mu(E)x] \, dE \quad (1)$$

In the case of Al foils, used in the experiment, the absorption coefficient $\mu(E)$ can be approximated in the range 2–50 keV [5] by

$$\mu(E) = 4.669E^{-2.82} = BE^{-\gamma} \quad (2)$$

where E is the photon energy in keV and (E) is in μm^{-1}. Following [4] the spectral distribution is given by

$$S_1(E_x) \approx -\frac{x}{c}\frac{dW(x)}{dx} \quad (3)$$

where c is a constant and E_x is determined from the relation

$$\mu(E_x)x = 1 \quad (4)$$

In this way, knowing the absorption function $W(x)$ one can derive the spectral distribution function $S(E)$. Using the least-squares method $W(x)$ was approximated by a third order polynomial

$$W(x) = A_0 + A_1x + A_2x^2 + A_3x^3 \quad (5)$$

From Equation 3 we obtain

$$S_1(E) = -\frac{1}{c}(A_1x + 2A_2x^2 + 3A_3x^3) \quad (6)$$

For x determined from Equations 4 and 2

$$S_1(E) = -\frac{1}{c}(A_1B^{-1}E^{\gamma} + 2A_2B^{-2}E^{2\gamma} + 3A_3B^{-3}E^{3\gamma}). \quad (7)$$

Using this method the spectral distribution of the pulse was calculated on the basis of the measured absorption data. Plotted in Fig. 3 are the normalized spectra obtained for a tungsten target and positive voltages of 10 kV, 15 kV, 20 kV, 25 kV and 30 kV, (curves 1, 2, 3, 4 and 5, correspondingly). A computer run, including the two 0.2 mm thick Be window transmissions gave no change in the

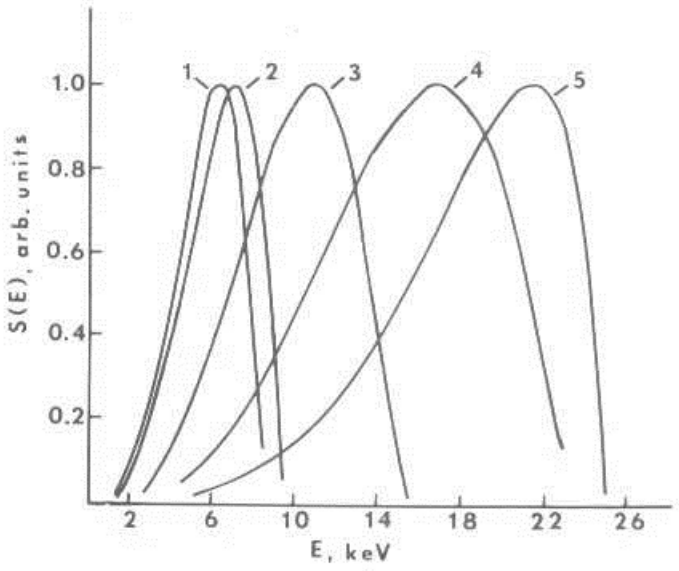

Figure 3 Normalized X-ray spectra of the pulse at different voltages, obtained using the filter technique: 1, 10 kV; 2, 15 kV; 3, 20 kV; 4, 25 kV; 5, 30 kV.

spectral distribution within the range of interest. The major attenuation of the beryllium foils is for softer spectral components under 1 keV, where line emission might be expected.

For the purpose of comparison the spectrum of a bremsstrahlung emission was also calculated. The spectral distribution function of the bremsstrahlung emission was approximated by the function

$$S_2^i(E) = A \exp(\alpha E) \sin(\beta E) \quad (8)$$

where $A = (2/3) \exp [-2\pi/(3\sqrt{3})]$ is a normalizing coefficient, $\alpha = \pi/(E_0\sqrt{3})$, $\beta = \pi/E_0$ and E_0 is the maximum energy in the spectrum. The approximation is chosen in such a way that $E_m = (2/3)E_0$ where E_m is the X-ray energy in the maximum of the the spectral distribution function, and E_0 (keV) = U (kV). Here U is the accelerating voltage.

Using the method described above, the integral energy $W_2(x)$ was calculated and the spectral distribution function $S_2^f(E)$ was restored. In this way one can check the accuracy of the method and find the distortions, if any, of the initial spectral distribution. Fig. 4 shows the initial spectral distribution function $S_2^i(E)$ (curve 1) and the final spectral distribution function $S_2^f(E)$ (curve 2). As seen from Fig. 4, the computer calculated curve 2 is a little narrowed and its maximum is slightly shifted towards the lower energies.

Given also in Fig. 4 is the spectral distribution function $S_1(E)$ (curve 3), calculated from the experimental data for the same applied voltage,

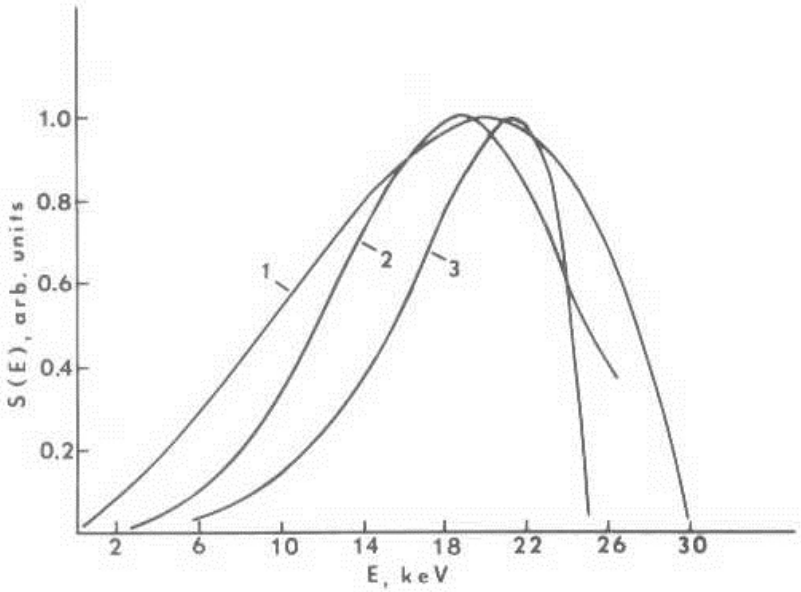

Figure 4 Comparison of the classical bremsstrahlung spectra and that experimentally measured by the filter technique at 30 kV. Curve 1, initial spectral distribution function $S_2^i(E)$ of the bremsstrahlung emission; 2, final spectral distribution function $S_2^f(E)$ of the bremsstrahlung emission, restored by the computer processing; 3, spectral distribution function $S_1(E)$, obtained from the experimental absorption data.

$U = 30$ kV, and a tungsten target. For comparison, all three curves are normalized to unity. The maximum of the experimental curve is shifted to higher energies compared to the bremsstrahlung function $S_2^f(E)$. More clearly, the difference between the bremsstrahlung and the experimentally obtained spectra is seen in Fig. 5. Plotted in the figure is the position of the maximum E_m of the spectral distribution versus applied voltage U. Curve 1 applies for the initial bremsstrahlung spectrum (Equation 8) $E_m = (2/3)U$ [6]. Curve 2 is obtained after computer processing of $S_2^i(E)$ and consequent restoring, i.e. $S_2^f(E)$ maximum position is plotted. A linear dependence in both cases is evident. However, the slope of curve 2 is slightly lower, $E_m = 0.626U$. On the contrary, the experimentally obtained dependence, curve 3, is not linear. A least squares fit gave $E_m = 0.0785U^{1.65}$.

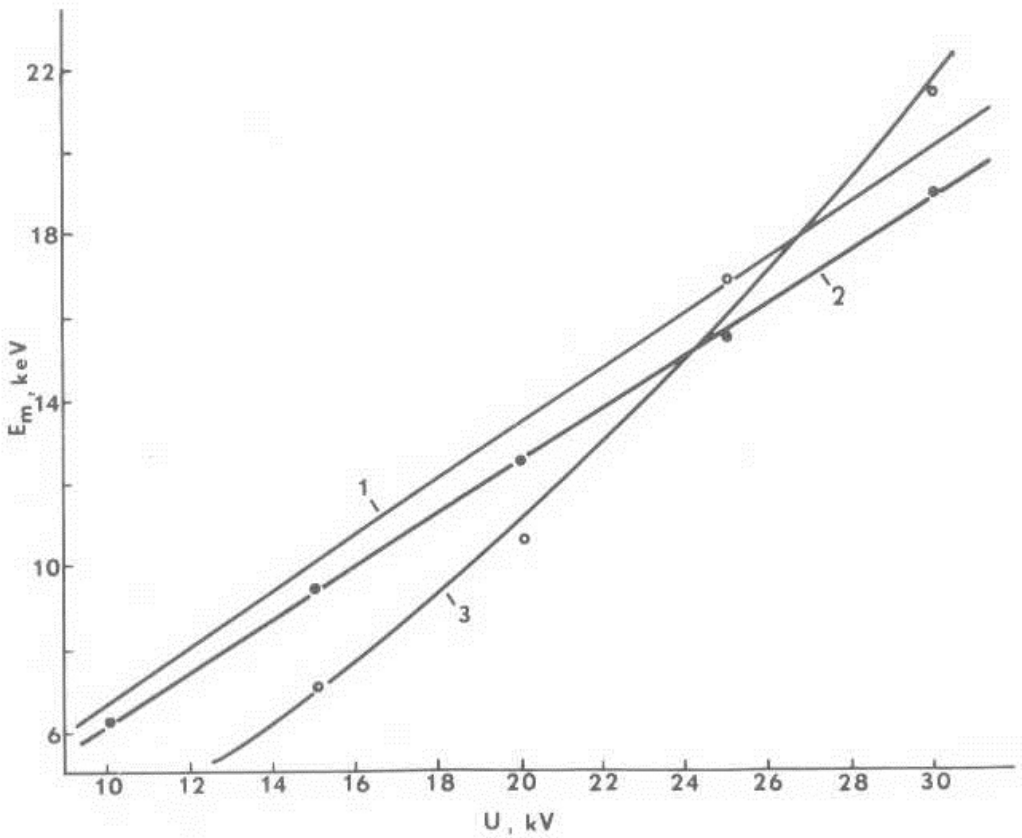

Figure 5 Dependence of the X-ray energy E_m in the maximum of the spectral distribution function on the applied voltage: 1, initial bremsstrahlung spectra; 2, final bremsstrahlung spectra after processing; 3, experimental spectra.

4. Discussion

The most important result in Figs. 3 and 5 is that the energy of the X-ray quanta is shifted gradually to the short-wavelength side as the interelectrode voltage increases. It is interesting to note that similar results were reported in vacuum spark discharge by Lie [7] and later discussed by Fukai and Clothiaux [8] and Benford [9].

The true mechanisms in the production of high energy X-ray radiation are difficult to deduce on the bases of the present experimental data. The trivial emission, mostly due to target bombardment of plasma electrons, seems to be inadequate, as shown by the measured spectra, Figs. 3–5. It is important to note in this connection the dependence of X-ray pulse amplitude A_1, A_2 on U, the magnitude of the applied voltage (Fig. 2 in [1]). The second pulse, caused by electron bombardment reveals a dependence of the type $A_2 \propto U^{3.6}$. In contrast, the amplitude of the first pulse depends on U as $A_1 \propto U^{3.1}$ with a sufficiently high correlation coefficient.

The basic process involved is probably laser plasma polarization in the strong electric field. Consequently, several mechanisms for X-ray production might be involved.

(a) Recombination of the polarized plasma.

(b) The high currents in the kiloampere region might lead to plasma instabilities of the kind observed in the linear pinch discharges [10, 11]. The micro-instabilities of the plasma may cause anomalous acceleration of electrons which interact with the plasma in a collective manner or hit the target.

(c) An increased photo-ionization cross-section [12] and/or enhanced absorption of the laser energy.

Acknowledgement

We thank N. Uluchev for technical assistance.

References

1. S. G. DINEV, CH. I. RADEV, K. V. STAMENOV and K. A. STANKOV, *Opt. Commun.* **30** (1979) 219–23.
2. GY. FARKAS and Z. GY. HORVATH, *ibid* **21** (1977) 408–10.
3. E. W. McDANIEL, 'Collision Phenomena in Ionized Gases' (John Wiley & Sons, New York, (1964).
4. P. J. MALLOZZI, H. M. EPSTEIN, R. G. JUNG, D. C. APPLEBAUM, P. P. FAIRAND and W. J. CALLAGHER, in 'Fundamental and Applied Laser Physics' *Proceedings of the Esfahan Symposium* (John Wiley & Sons, 1971). p. 165.
5. O. F. NEMETZ and U. V. GOFMAN, 'Handbook of Nuclear Physics' (Naukova Dumka, Kiev, 1975).
6. G. S. SAMOILOVITCH, 'Handbook of Nondestructive control' (Mashinostroenie, Moscow, 1976).
7. T. N. LIE, *Astrophys J.* **190** (1974) 467–70.
8. J. FUKAI and E. J. CLOTHIAUX, *Phys. Rev. Lett.* **34** (1975) 863–66.
9. G. BENFORD, *Appl. Phys. Lett.* **33** (1978) 983–84.
10. T. N. LIE and R.C. ELTON, *Phys. Rev. A* **3** (1971) 865–71.
11. J. SHILOH, A. FISHER and N. ROSTOKER, *Phys. Rev. Lett.* **40** (1978) 515–18.
12. V. S. LETOKHOV, V. I. MISHIN and A. A. PURETSKY, *Prog. Quant. Elect.* **5** (1977) 139.